Research on Engineering Structures & Materials
journal homepage: http://www.jresm.org
Research Group

Technical Note

On the effect of numerical parameters in finite element through thickness modeling for springback prediction

Bora Şener[1.a], Toros Arda Akşen[2.b], Emre Esener[3.c], Mehmet Fırat[*2,d]

[1]*Department of Mechanical Engineering, Yildiz Technical University, Istanbul, Turkey*
[2]*Department of Mechanical Engineering, The University of Sakarya, Sakarya, Turkey*
[3]*Department of Mechanical Engineering, Bilecik Seyh Edebali University, Bilecik, Turkey*

Article Info

Article history:

Received 8 Mar 2022
Revised 9 May 2022
Accepted 16 May 2022

Keywords:
Springback;
TWIP980 steel;
U-Bending;
Finite Element Method

Abstract

The usage of advanced high strength steels (AHSS) presents important advantages in the reduction of the car body weight. However, these steels exhibit high springback behavior and causes to several problems in the manufacturing. Therefore, the prediction of the springback for AHSS is an important engineering task. In this study, the effect of numerical parameters in finite element through thickness modelling for springback prediction was investigated. U-draw bending process of transformation-induced plasticity-TWIP980 steel was performed as benchmark study. In the study, both shell and solid elements were taken into account. Number of integration points for shell elements and number of elements along the thickness direction for solid elements were evaluated. As a result, 5 integration points were determined as optimum value for shell elements however similar predictions results were obtained between the shell and solid elements.

© 2022 MIM Research Group. All rights reserved.

1. Introduction

Springback can be defined as deviation from the designed target shape after removal of the load. This phenomenon causes to difficulties in the subsequent manufacturing processes and assembly of the parts [1]. Accurate prediction of springback by finite element analysis (FEA) is a complicated task since numerous numerical and process parameters have effect on the prediction accuracy of springback. An accurate finite element modeling of a stamping process eliminates time-consuming stages especially at die compensation procedure [2-4]. From this perspective, finite element modelling stages must be well defined and optimized by means of accuracy and solution time. A great number of calculation parameters in finite element simulations effects the accuracy and the solution time of the simulation [5, 6]. Mesh design of the geometries and plasticity modeling steps dominates the accuracy of the simulations [7-9]. Mesh design generally includes element type, element number, and number of integration points (for shell elements). In the literature, Lee and Yang [10] investigated the effect of contact damping, penalty parameters, mesh size in the blank, number of elements on tool corners and punch velocity on springback prediction. They performed finite element (FE) simulations of U bending process with different values of the mentioned numerical parameters and determined that mesh size in the blank and number of elements on tool corners are the most important factors influencing springback prediction. Xu et al. [11] studied the effect of nodal damping value, number of integration point, mesh size in the blank and punch velocity on springback prediction of U bending process and determined the optimum values of the

*Corresponding author: firat@sakary.edu.tr
[a] orcid.org/0000-0002-8237-1950; [b] orcid.org/0000-0002-7087-3216; [c] orcid.org/0000-0001-5854-4834; [d] orcid.org/0000-0002-3973-4736
DOI: http://dx.doi.org/10.17515/resm2022.415st0308tn

numerical parameters. Chen et al. [12] performed finite element (FE) simulations of slit-ring cup and three automotive parts, namely fender load beam, a rail and a cross member in dynamic-explicit finite FE program Ls-Dyna. They studied the effect of mass scaling, contact method and material model on springback prediction. Authors determined that accuracy of springback prediction is improved by using selective mass scaling, smooth contact method and Yoshida-Uemori [13] nonlinear isotropic-kinematic hardening model. Yao et al. [14] investigated the effect of loading curve, mesh size, number of through thickness integration points and mass scaling factor. They determined that the decreasing of punch velocity, increasing of adaptivity level and number of integration points improve the springback prediction accuracy. Trzepiecinski and Lemu [15] researched the influence of a number of integration points, integration rule, the orientation of the blank and friction coefficient on the amount of springback in V bending process. From the numerical results, they determined that minimum five elements through the thickness direction for Gauss's integration rule are required to obtain compatible results, while similar results were obtained both Gauss and Simpson rules with seven or nine integration points. A comprehensive study was carried out by Firat et al. [16]. They investigated the effects of both numerical and process parameters on the springback prediction accuracy of U bending and an engine suspension bracket. The effects of element size and punch speed from numerical parameters and blank holder force (BHF), draw bead penetration and friction coefficient from process parameters were evaluated in their study. The interactions between the parameters and their effects on the springback and thinning behavior were determined by multi-linear regression and the optimum parameters were presented. Esener et al. [17] performed a sensitivity analysis for stamping process of a roof stiffener part manufactured from dual phase-DP600 steel and determined optimum numerical and process parameters which minimize the amount of springback. They investigated number of integration points through the thickness direction, shell element formulation, friction coefficient and BHF values and found the optimum parameters by using meta-model-based design of experiment.

As it seen from the literature studies, the effect of integration points through thickness was evaluated by several researchers in the past [10, 11, 14, 15]. However, comparisons were generally restricted to only the performance of the mesh sizes. The solution times were mostly ignored for the determination of the optimum mesh size. This study investigated the effect of the mesh size on spring-back prediction in terms of prediction performance and solution times. Moreover, an implicit solver was utilized in this work which is rare because explicit solvers have been preferred extensively for spring-back prediction due to the lower solution times.

On the contrary, implicit solvers have to calculate the stiffness matrix at all increments of the simulation, which increases the solution time. Therefore, implicit solvers provide consistent results for applications of plasticity. In addition, this study focuses on the effect of an anisotropic yield criterion on spring-back prediction. Although the influence of kinematic hardening is well known [13], the influence of the anisotropic yield criterion on spring-back prediction was not extensively investigated.

It can be seen that there is numerous studies that models the blank geometry using shell and solid elements. However, investigation of solid element number trough the material thickness and number of integration points in shell elements for springback predictions is a challenge for process engineers. For this reason, presented study focused on finite element through thickness modelling for springback prediction. In this study, springback of TWIP980 sheet from advanced high strength steel (AHSS) was investigated by considering anisotropic plasticity model. U-draw bending process was performed and this process evaluated by using solid and shell elements with different trough thickness

modeling parameters. Finite element (FE) analyses were performed with a commercial implicit FE code and the predicted results were compared with experimental results.

2. Material and Method

In this study, U-draw bending process from the Numisheet93 benchmark is performed. Die tool geometries can be seen in Fig. 1. TWIP980 steel was used as material. TWIP steels consist of high manganese content and therefore it is fully austenitic at ambient temperature. The plastic deformation of this steel is carried out by both twinning and dislocation slip mechanisms [18]. Mechanical properties of the material can be seen in Table 1.

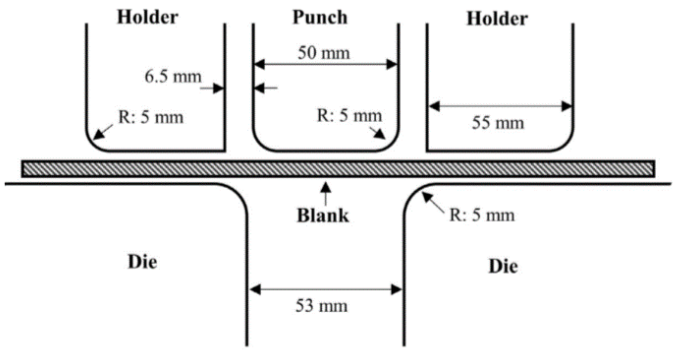

Fig. 1 Tool dimensions for U-draw bending [20]

Table 1. Mechanical properties of TWIP980 steel [20]

Angle (^{0})	Young modulus (MPa)	Yield Stress (MPa)	r-value
0^0	207000	941.1	0.678
45^0		896.9	1.147
90^0		938.8	1.279

According to the additive plasticity approach, strain increment can be decomposed into the elastic and plastic components, as seen in Eq. (1).

$$d\varepsilon_{ij} = d\varepsilon_{ij}^{e} + d\varepsilon_{ij}^{p} \tag{1}$$

Cauchy stress tensor components can be decomposed into deviatoric and hydrostatic parts.

$$d\sigma_{ij} = dS_{ij} + d\sigma_m I \tag{2}$$

The deviatoric part is responsible for the shape-changing, while the hydrostatic part is responsible for the volume change. σ_m and I represent the mean stress and Kronecker delta, respectively. Eq. (3) establish a correlation between the elastic strain component and the deviatoric stress components.

$$dS_{ij} = 2Gd\varepsilon_{ij}^{e} \tag{3}$$

Ultimately, the yield criterion separating the elastic and plastic regions from each other in stress space can be expressed by Eq. (4).

$$f(\sigma_{ij}) = \sigma_{eqv}(\sigma_{ij}) - \sigma_0(\varepsilon_{ij}^p) = 0 \quad (4)$$

In this study, initial anisotropy of the material was defined with orthotropic quadratic Hill48 yield criterion [21] and the relationship between the plastic strain increments and stresses was defined with associated flow rule. The criterion has six coefficients for three-dimensional stress state and it could be written as follows:

$$f(\sigma_{ij}) = \{(F(\sigma_{22} - \sigma_{33})^2 + G(\sigma_{33} - \sigma_{11})^2 + H(\sigma_{11} - \sigma_{22})^2 + 2L{\sigma_{23}}^2 + 2M{\sigma_{13}}^2 + 2N{\sigma_{12}}^2\}^{1/2} \quad (5)$$

where F, G, H, L, M and N are constants which define anisotropy. In this study, Lankford based identification was considered and F, G, H and N were determined by following equations. The remaining coefficients L and M were used as 1.5 due to neglecting of anisotropy along thickness direction.

$$F = \frac{r_0}{r_{90}(1+r_0)}, \quad G = \frac{1}{1+r_0}, \quad H = \frac{r_0}{1+r_0}, \quad N = \frac{(r_0+r_{90})(1+2r_{45})}{2r_{90}(1+r_0)} \quad (6)$$

r_0, r_{45} and r_{90} denote Lankford coefficients along the three main directions. Hill48 plasticity model coefficients were given in Table 2 for TWIP980 steel. Prediction performance of the Hill48 model was evaluated with directionality estimations for TWIP980 steel. Fig. 2 illustrates the r value, the yield stress ratio and the yield surface predictions of Hill48 plasticity model for TWIP980 steel.

Table 2. Hill48 coefficients of TWIP980

F	G	H	L	M	N
0.316	0.596	0.404	1.5	1.5	1.502

The experimental r values were accurately captured as expected (Fig. 1a). Nevertheless, some deviations were seen between the analytical yield ratio predictions and the experimental ones (Fig 1b). The associated flow rule (AFR) was employed to establish a relation between the Cauchy stress components and plastic strain components, and the AFR is given in Eq. (7).

$$d\varepsilon_{ij}^p = d\lambda \frac{df}{d\sigma_{ij}} \quad (7)$$

In the equation above, $d\lambda$ is the proportionality factor. In the study, isotropic hardening assumption and was considered and hardening of the material was defined with Swift hardening law. The hardening parameters are given in Table 3 and the Swift law was given in Eq. (8).

$$\sigma = K(\varepsilon_0 + \varepsilon_p)^n \quad (8)$$

Table 3. Swift model parameters of TWIP980 [20]

K(MPa)	ε_0	n
2349.9	0.167	0.502

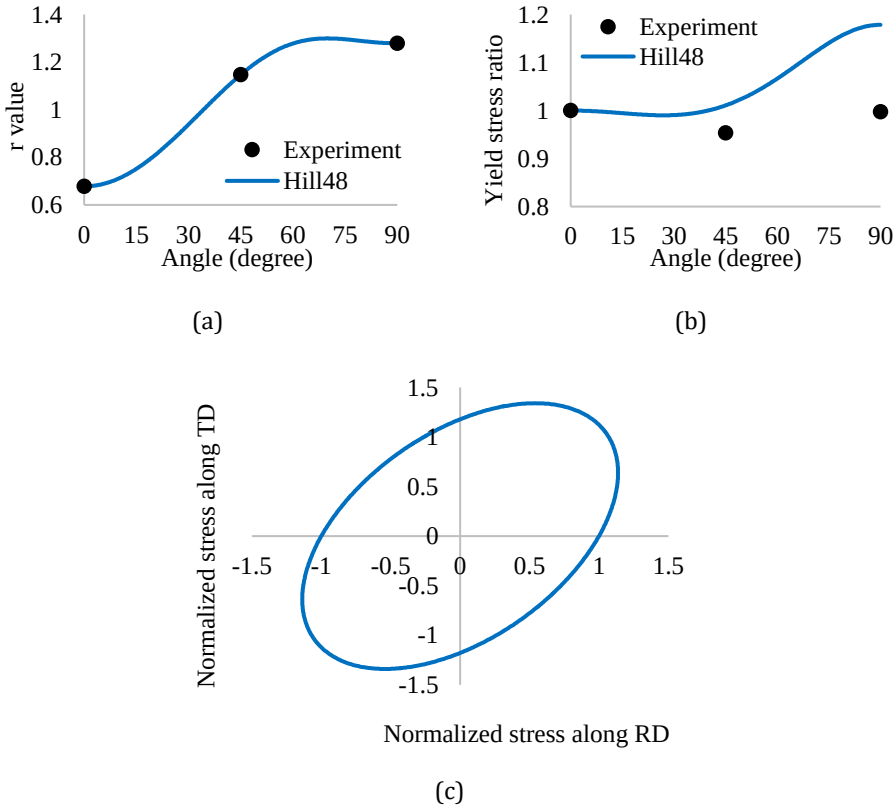

Fig. 2 (a) r value, (b) yield stress ratio, (c) yield surface predictions of the Hill48 criterion for TWIP980 steel

3. Application Study

In this study, U-draw bending process was modeled with implicit FE code Marc [21]. Blank part was modeled as deformable body, while other die tools were modeled as rigid body. Control nodes were assigned for punch and blank holder so as to apply the necessary boundary conditions. In simulations, two element types were considered, and blank was separately meshed with shell and solid elements. Bilinear, four-node fully integrated shell elements, including transverse shear effects, were adopted for shell element formulation. On the other hand, fully integrated hexahedral constant dilatational elements were used for solid element formulation. Both elements are free from shear locking [21, 22]. In the first case, 1, 2, 3, and 4 solid elements were used through the thickness and in the second case shell elements with 3, 5, 7 and 9 integration points were evaluated. For both element type, half of the geometry was modelled due to symmetry conditions. The Coulomb bilinear friction model was employed, and the friction coefficient between the blank and the tools was assumed to be 0.13 [20]. Node to segment contact algorithm coupled with penalty factor was utilized to eliminate the penetration. The FE model of the process was shown in Fig 3. In the FE model, blank holder force was assigned as 10 kN, 25 kN, and 50 kN separately and the punch displacement was performed as 70 mm.

Cross section of the deformed geometry was investigated following FE analyses, and three parameters were taken into account for springback measurement recommended in the literature studies that used U-draw bending [23, 24]. θ_1 and θ_2 angles and the sidewall

radius (ρ) can be seen in Fig. 4. θ_1, θ_2 and ρ parameters were predicted for each FE analysis and the results were compared with experiments obtained in Numisheet93 benchmark. The comparison between the numerical and experimental results for shell and solid elements were shown in Fig. 5 and Fig. 6, respectively.

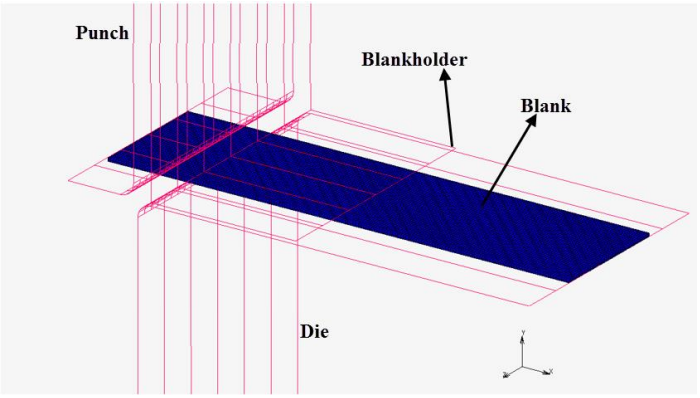

Fig. 3 FE model of U-draw bending

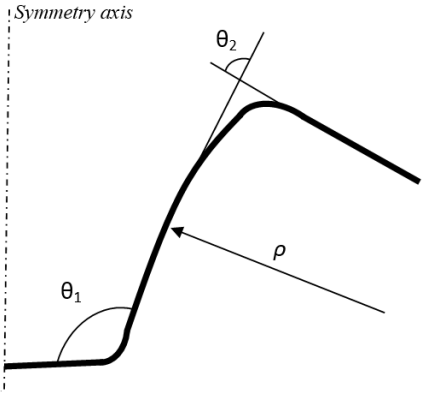

Fig. 4 Springback parameters in U-draw bending process

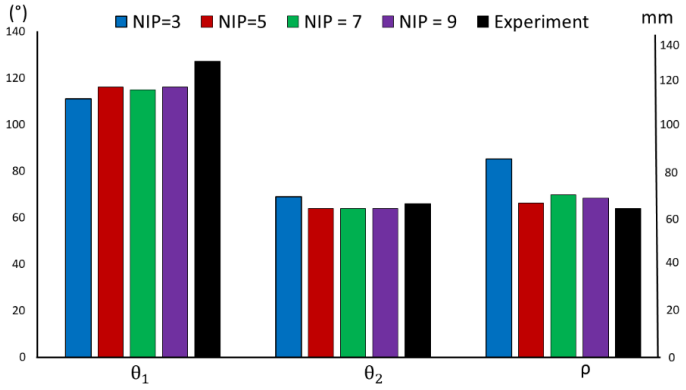

Fig. 5 Comparison results for shell elements with different integration point numbers

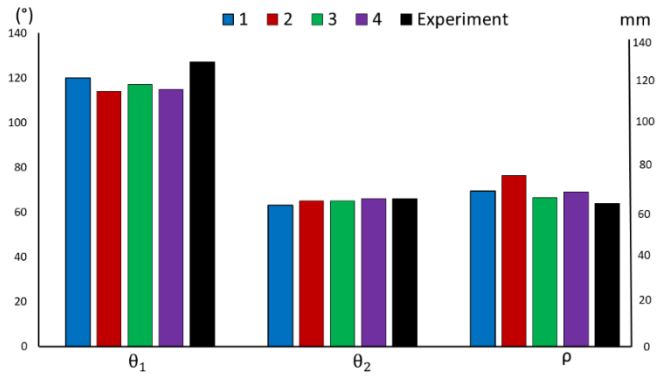

Fig. 6 Comparison results for different number of solid elements that used trough the thickness

It can be seen from the figures, for shell elements, no significant differences were observed between the predicted and experimental springback angles (θ1–θ2) when the more than 5 integration points were used. However, minor differences were observed for sidewall radius. When it comes to solid elements, it was observed that increasing of the number of elements in thickness direction has not an important effect on the prediction accuracy of springback for U-draw bending process. The solution times of different element numbers and integration points through-thickness directions were also compared, and Table 4 shows the CPU solution times.

Table 4. CPU solution times

Solid	Element Number	1	2	3	4
	Solution Time (s)	6424.86	11106.77	11805.89	13856.98
	Iteration (Cycle)	2816	2694	2367	2135
Shell	NIP	3	5	7	9
	Solution Time (s)	6564.08	4149.25	5418.34	10902.21
	Iteration (Cycle)	2818	1865	2016	2132

It was observed that higher solution times were obtained for the simulations with the solid element formulation. In addition, the solution times increase with the increase in through-thickness element number or NIP. However, for the results obtained by the 3 NIP in thickness, the solution time was increased. It may be a consequence that the models have difficulty converging because the total iteration number of 3 NIP was considerably higher than the others. Correspondingly, an increase in the NIP through-thickness may lead to an improvement in the convergence performance. Moreover, for shell element formulation, after the 3 NIP iteration numbers suddenly decreased and from 5 NIP to 9 NIP, iteration numbers increased.

The equal number of integration layers in thickness was considered to properly compare the performances of shell element and solid element formulations. From this point of view, the FE models with 2 elements in thickness for solid and 5 NIP through-thickness for shell element formulations were selected for further studies. In order to evaluate the performance of the Hill48 criterion on the spring-back prediction, U draw bending simulations were carried out for BHF 10 kN and 25 kN as well. The results were compared with the experimental results and literature studies [20]. Fig 7 demonstrates the numerical and experimental spring back outcomes for 10 kN, 25 kN, and 50 kN BHF.

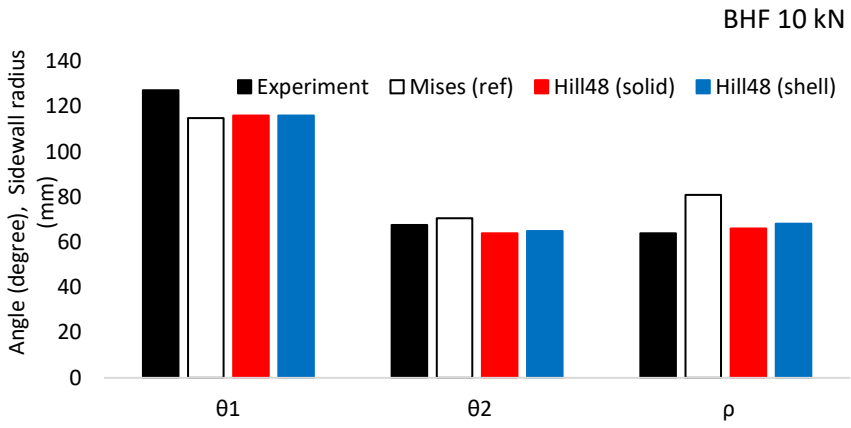

(a)

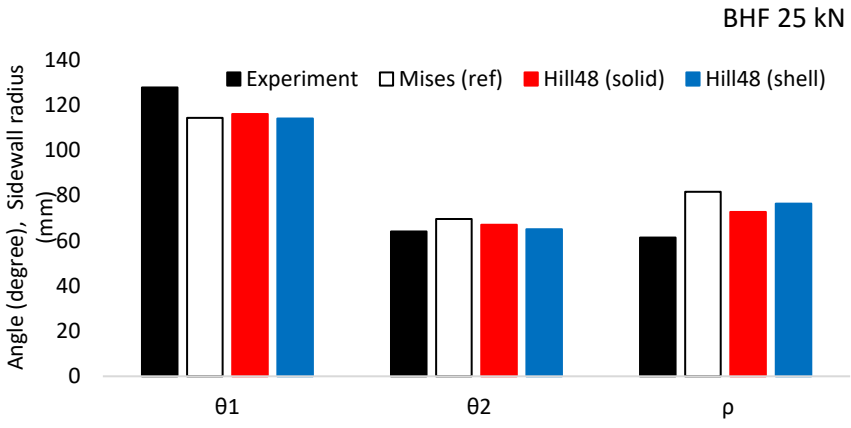

(b)

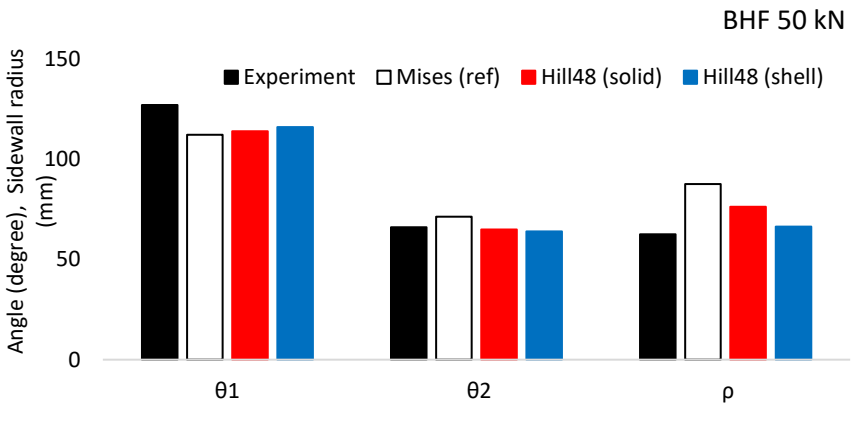

(c)

Fig. 7 Springback parameters for a) BHF = 10 kN, b) BHF = 25 kN, c) BHF = 50 kN

The von Mises results were taken from the Ref. [20]. Hill48 results obtained by solid and shell element formulations were compared with the reference Mises results and experimental results simultaneously. For all BHF values, Mises overpredicted the θ_1 while underpredicted the θ_2 and ρ. On the other hand, Hill48 results for both element formulations improved prediction performance and better agreed with the experimental results for all spring back parameters. However, a slight difference between both element formulations of Hill48 was observed. Shell element formulation was found to be more suitable and practical for spring-back prediction when considering the CPU solution times.

4. Conclusions

In this study, the effect of FE parameters on the prediction accuracy of the springback was investigated. U-draw bending process was selected as benchmark study and springback of TRIP980 sheet from AHSS was predicted with implicit FE code Marc. Element type, NIP, the number of elements in thickness direction were taken as variables and FE analyses were performed with different numerical parameters and different BHF values. Two angles between the sidewall and the deformed profile and also sidewall radius was selected as springback measurement. The predicted results from FE analyses were compared with experimental results and numerical results obtained from the literature study. The conclusions are as follows.

- It was found from the comparisons that increasing of NIP has no significant effect on the springback angle predictions. However, only minor differences were observed in sidewall radius predictions.
- It was determined that the usage of 5 integration points through the thickness direction was adequate for shell elements. When comparing the CPU solution times, the model with 5 NIP was found to be lower than the others. This situation is attributed to the improved convergence performance.
- Significant differences between the predictions were not observed when the number of elements in thickness direction increased for solid elements. When the solution times were regarded, a noticeable difference was not observed for different element numbers through the thickness.
- Simulations were repeated for different BHF values using solid, and shell element formulations utilizing the models with the optimum element numbers and NIP through the thickness. The models with 2 elements and 5 NIP through-thickness for solid and shell element formulations were selected for these analyses. Numerical results were compared with the experimental results and reference isotropic criterion results. The prediction accuracy was enhanced for both element formulations when the Hill48 criterion was employed.
- A noticeable difference was not observed between the solid and shell element formulations in terms of predicted spring back angles and sidewall radius. However, shell element formulation was found to be more practical and suitable for spring-back prediction in terms of CPU solution times.

References

[1] Wagoner RH, Lim H, Lee M-G. Advanced issues in springback. International Journal of Plasticity, 2013; 45: 3-20. https://doi.org/10.1016/j.ijplas.2012.08.006

[2] Zhang L, Li, H, Bian T, Wu C, Gao Y, Lei C. Advances and challenges on springback control for creep age forming of aluminum alloy. Chinese Journal of Aeronautics, 2021. https://doi.org/10.1016/j.cja.2021.10.019

[3] Wang H, Zhou J, Zhao TS, Liu LZ, Liang Q. Multiple-iteration springback compensation of tailor welded blanks during stamping forming process. Materials & Design, 2016; 102: 247-254. https://doi.org/10.1016/j.matdes.2016.04.032
[4] Jianjun WU, Zhang Z. An improved procedure for manufacture of 3D tubes with springback concerned in flexible bending process. Chinese Journal of Aeronautics, 2021; 34(11): 267-276. https://doi.org/10.1016/j.cja.2020.05.036
[5] Navarro M, Ivorra S, Varona, FB. Parametric finite element analysis of punching shear behaviour of RC slabs reinforced with bolts. Computers & Structures, 2020; 228, 106147. https://doi.org/10.1016/j.compstruc.2019.106147
[6] Greve L, van de Weg B. Surrogate modeling of parametrized finite element simulations with varying mesh topology using recurrent neural networks. Array; 2022; 14: 100137. https://doi.org/10.1016/j.array.2022.100137
[7] Jiang HJ, Ren YX, Lian JW, Xu WL, Gao NH., Wang XG, Jia CS. A new predicting model study on U-shaped stamping springback behavior subjected to steady-state temperature field. Journal of Manufacturing Processes, 2022; 76: 21-33. https://doi.org/10.1016/j.jmapro.2022.02.004
[8] Yoshida F. Description of elastic-plastic stress-strain transition in cyclic plasticity and its effect on springback prediction. International Journal of Material Forming, 2022; 15(2): 1-17. https://doi.org/10.1007/s12289-022-01651-1
[9] Solfronk P, Sobotka J, Koreček D. Effect of the Computational Model and Mesh Strategy on the Springback Prediction of the Sandwich Material. Machines, 2022; 10(2): 114. https://doi.org/10.3390/machines10020114
[10] Lee SW, Yang DY. An assessment of numerical parameters influencing springback in explicit finite element analysis of sheet metal forming process. Journal of Materials Processing Technology, 1998; 80-81: 60-67. https://doi.org/10.1016/S0924-0136(98)00177-0
[11] Xu WL, Ma CH, Li CH, Feng WJ. Sensitive factors in springback simulation for sheet metal forming. Journal of Materials Processing Technology, 2004; 151: 217-222. https://doi.org/10.1016/j.jmatprotec.2004.04.044
[12] Chen X, Shi M, Zhu X, Du C, Xie ZC, Xu S, Wang C-T. Springback prediction improvement using new simulation technologies. SAE Technical Paper Series, 2009. https://doi.org/10.4271/2009-01-0981
[13] Yoshida F, Uemori T. A model of large-strain cyclic plasticity describing the Bauschinger effect and work hardening stagnation. International Journal of Plasticity, 2002; 18; 661-686. https://doi.org/10.1016/S0749-6419(01)00050-X
[14] Yao H, Liu SD, Du C, Hu Y. Techniques to improve springback prediction accuracy using dynamic explicit FEA codes. SAE Technical Paper Series, 2002. https://doi.org/10.4271/2002-01-0159
[15] Trzepiecinski T, Lemu HG. Effect of computational parameters on springback prediction by numerical simulation. Metals, 2017; 7: 1-14. https://doi.org/10.3390/met7090380
[16] Firat M, Mete OH, Kocabicak U, Ozsoy M. Stamping process design using FEA in conjuction with orthogonal regression. Finite Elements in Analysis and Design, 2010; 46; 992-1000. https://doi.org/10.1016/j.finel.2010.07.005
[17] Esener E, Ercan S, Firat M. (2014) A Sensitivity analysis by using design of experiment and its application in stamping. An International Conference on Engineering and Applied Sciences Optimization, Kos Island, Greece, June, 2008.
[18] Grassel O, Kruger L, Frommeyer G, Meyer LW. High strength Fe-Mn-(Al, Si) TRIP/TWIP steels development-properties-application. International Journal of Plasiticity, 2000; 16: 1391-1409. https://doi.org/10.1016/S0749-6419(00)00015-2
[19] Makinouchi A, Nakamachi E, Onate E, Wagoner R. Numerical simulation of 3-D sheet metal forming proceses verification of simulation with experiment. Proceedings of the 2nd International Conference Numisheet'93, Isehara, Japan, September, 1993.

[20] Choi J, Lee J, Bong HK, Lee M-G, Barlat F. Advanced constitutive modeling of advanced high strength steel sheets for springback prediction after double stage U-draw bending. International Journal of Solids and Structures, 2018; 151: 152-164. https://doi.org/10.1016/j.ijsolstr.2017.09.030
[21] Marc (2018) 2008.1 Volume A: Theory and User Manual.
[22] Marc (2018) 2008.1 Volume B: Element Library.
[23] Hill R. A theory of the yielding and plastic flow of anisotropic metals. Proc. Soc. London A, 1948; 193A: 291-297. https://doi.org/10.1098/rspa.1948.0045
[24] Nakamachi E. Guide to the benchmark test - simulation and experiment. In: Makinochi A, Nakamachi E, Onate E, Wagoner RH, editors. Numisheet93. Tokyo: The Institute of Physical and Chemical Research, 1993; 32-39.